Desalination and Water Treatment
www.deswater.com
doi: 10.1080/19443994.2014.917988

54 (2015) 944–955
April

Taylor & Francis
Taylor & Francis Group

Utilization of self-synthesized ZnO nanoparticles in MPR for industrial dye wastewater treatment using NF and UF membrane

Nur Hanis Hayati Hairom[a,c], Abdul Wahab Mohammad[b,*], Law Yong Ng[a], Abdul Amir Hassan Kadhum[b]

[a]*Faculty of Engineering and Built Environment, Department of Chemical and Process Engineering, Universiti Kebangsaan Malaysia, 43600 UKM Bangi, Selangor, Malaysia, emails: nurhanishayati@gmail.com (N.H.H. Hairom), nglawyong@gmail.com (L.Y. Ng)*
[b]*Faculty of Engineering and Built Environment, Centre for Sustainable Process Technology (CESPRO), Universiti Kebangsaan Malaysia, 43600 UKM Bangi, Selangor, Malaysia, emails: wahabm@eng.ukm.my (A.W. Mohammad), amir@eng.ukm.my (A.A.H. Kadhum)*
[c]*Faculty of Engineering Technology, Department of Chemical Engineering Technology, Universiti Tun Hussein Onn Malaysia, 86400 Parit Raja, Batu Pahat, Johor, Malaysia*

Received 27 December 2013; Accepted 17 April 2014

ABSTRACT

This study attempted to use zinc oxide (ZnO) nanoparticles in membrane photocatalytic reactor (MPR) for industrial dye wastewater treatment. Performance comparison of nanofiltration (NF) and ultrafiltration (UF) in the MPR system were investigated to produce cleaner discharge and to retain the ZnO for reuse. From the results, the optimum operational condition of MPR occurred under pH 11 and 0.1 g L^{-1} of ZnO loading. NF membrane performance improved after the addition of ZnO nanoparticles in the wastewater; in terms of normalized flux reduction (65%), colour removal (100%), chemical oxygen demand (92%), turbidity reduction (100%) and total suspended solid rejection (100%). In contrast, UF membrane showed worse performance, due to the permeation of dye molecules and nanosized ZnO across the UF membrane pores. Membrane characterizations of field emission scanning electron microscopy and energy dispersive X-ray results confirmed that the ZnO nanoparticles and NF membrane application has a great potential for improving MPR system in industrial wastewater treatment.

Keywords: Zinc oxide nanoparticles; Membrane photocatalytic reactor; Nanofiltration; Ultrafiltration; Industrial dye wastewater

1. Introduction

Newsprint printing industry is one of the world's most important manufacturing. The main environmental issue arises from the newsprint industry is generation of wastewater due to the consumption of large amounts of water during the printing process. Generally, the wastewater produced from this industry is characteristically high in both colour and organic content, consist of complex components, heavily contaminated and difficult

*Corresponding author.

Presented at the 6th International Conference on the "Challenges in Environmental Science and Engineering" (CESE-2013), 29 October–2 November 2013, Daegu, Korea

to be biodegraded [1,2]. It has also been known as aesthetically displeasing and most of the pigments are toxic and mutagenic. These undesirable properties will affect the biological process in the stream due to the lack of dissolved oxygen and obstruction of sunlight penetration [3]. In addition, printing and dyeing wastewater is not only disrupting the aquatic communities, but also bring some hazards that pose a risk to the environment and human health. Conventional wastewater treatment methods (physical, biological or chemical) were typically applied to this industry. However, there are several limitations of these methods to meet the discharge criterion of environmental quality. Therefore, development of more advanced technologies is particularly required for better effluent discharge, principally to attain environmental cleanliness and human health safety.

In recent years, photocatalytic degradation processes with application of nanoparticles as a photocatalyst has become attractive for dye wastewater treatment due to its efficiency of dye degradation [4–6]. In this process, hydroxyl radicals (·OH) are generated as soon as the photocatalyst is illuminated by ultraviolet (UV) light. Consequently, the dyes are degraded and organic compounds are reduced to carbon dioxide (CO_2), clean water (H_2O) and inorganic constituents. Different nanoparticles have been used in photocatalysis studies including titanium dioxide (TiO_2), zinc oxide (ZnO), tin dioxide (SnO_2), zinc sulphide (ZnS), cadmium sulphide (CdS), iron oxide (Fe_2O_3), etc. for various types of wastewater treatment. Despite the efficiency of the nanoparticles to decompose the dyes and toxins in the wastewater; the most critical limitation is related to the separation of photocatalyst nanoparticles from the treated water after photodegradation process [7].

In order to solve the problem, photocatalysis coupled with membrane filtration systems have been intensively studied, which has led to the development of membrane photocatalytic reactors (MPRs). In this configuration, the membrane would act as a barrier for the photocatalyst and some molecules/ions from being transported along with the treated water in the final stream [8]. Other important advantages are simple configuration, reduction in the installation size, energy saving, better control of the residence time, efficient use of the UV light and photocatalyst, continuous process whereby the catalyst and products can be separated simultaneously, and high possibility to reuse the photocatalyst for further runs [7,9].

To date, more attention has been focused on the utilization of TiO_2 as the photocatalyst in MPR due to its chemical stability, excellent optical and electrical properties, strong redox ability and availability at low cost [10–12]. However, some literatures claimed that ZnO is better than TiO_2 in certain photocatalytic degradation process [13,14]. ZnO is a semiconductor with a wide bandgap similar to TiO_2 (~3.4 eV). The stable wurtzite crystal structure of ZnO has large exciton binding energy (60 meV) that can provide efficient UV light at room temperature. These characteristics have made ZnO as an attractive photocatalyst in the air/wastewater treatment by photodegradation mechanism. Furthermore, ZnO has been extensively used as a photocatalyst due to higher reactivity and surface area, photosensitivity, chemical stability, non-toxic nature, catalytic activity, tuneable nature of their optical and relatively low cost [15,16]. Based on these considerations, the effectiveness of ZnO in MPR needs to be explored in order to allow selection of appropriate photocatalyst for the coupling system. To the best of our knowledge, there has been no study dedicated for the use of ZnO photocatalysts in MPR. Previously, Kanade and colleagues [17] reported that the particle size and preparation methods of ZnO greatly influence the characteristics and performance of ZnO. The report was verified by recent studies, which confirmed that the photocatalytic activity of ZnO nanoparticles is very sensitive to precursors and synthesis process conditions [18]. Therefore, it is very important to produce much smaller size of ZnO through a virtuous method in order to acquire better performance during the photocatalysis process in MPR.

Over the years, various methods have been implemented for producing ZnO nanoparticles such as sonochemical [19], precipitation [17,18], electrolysis [20] and hydrothermal synthesis [21]. Among these preparation methods, precipitation has been recognized to be the preferable technique since it provided a simpler route, economic and occurs at a moderately low temperatures [17,18]. However, very limited study involving the synthesis of ZnO nanoparticles via precipitation method has been reported. Therefore, this study attempts to self-synthesis ZnO nanoparticles via precipitation method in order to produce more effective of photocatalyst in MPR.

The interest in using pressure-driven membrane processes, including microfiltration (MF), ultrafiltration (UF) and nanofiltration (NF) in the MPR coupling system has grown visibly due to their potential in resolving the problem concerning photocatalyst separation. Among these processes, NF membranes have shown the best performance and produce the highest quality of permeate whereas significant membrane

fouling is observed in MF and UF membrane [7]. In addition, small particles/molecules/ion can pass easily through the MF and UF membranes, leading to lower quality of permeate. Thus, in this study, performance comparison of NF and UF membrane in MPR is among the objectives. Literatures claimed that the polypiperazine amide NF and polyamide UF membrane have excellent performance and favourable economics [22–24]. However, very few studies are available on utilization of these membranes in MPR, mainly for industrial dye wastewater treatment.

Therefore, the focus of this work was primarily to study the efficiency of self-synthesized ZnO nanoparticles as the photocatalyst in MPR for industrial dye wastewater treatment. The ZnO nanoparticle was self-synthesized via a simple precipitation method; and the commercial ZnO nanoparticle was also used for comparison purposes. Two different types of membranes (polypiperazine amide NF and polyamide UF) were used in the MPR in order to investigate their performances for attaining high quality of permeates and membrane fouling mitigation.

1.1. Proposed photocatalytic degradation mechanism of dye wastewater

In order to understand the degradation of dye wastewater during the photocatalysis process in MPR, the proposed photocatalytic degradation mechanism of dye was described in Fig. 1.

The degradation process was started by photoexcitation of the ZnO, followed by the creation of an electron-hole pair on the nanoparticles surface:

$$ZnO + h\nu \rightarrow ZnO(eCB^- + hVB^+) \quad (1)$$

The direct oxidation of dyes occurred due to the high oxidative potential of the hole (hVB^+) in ZnO:

$$hVB^+ + \text{dye} \rightarrow \text{oxidation of dye} \quad (2)$$

Very reactive hydroxyl radicals were formed by the decomposition of water (Eq. (3)) or by the reaction between hole and hydroxide ion (Eq. (4)). The hydroxyl radical was extremely unstable which then lead to the degradation of organic chemicals [25].

$$hVB^+ + H_2O \rightarrow H^+ + {}^{\cdot}OH \quad (3)$$

$$hVB^+ + OH^- \rightarrow {}^{\cdot}OH \quad (4)$$

The molecular oxygen was reduced to superoxide anion by electron in the conduction band (eCB^-):

$$eCB^- + O_2 \rightarrow {}^{\cdot}O_2^- \quad (5)$$

The radical may form organic peroxides in the presence of organic scavengers (Eq. (6)) or hydrogen peroxide (H_2O_2) (Eq. (7)):

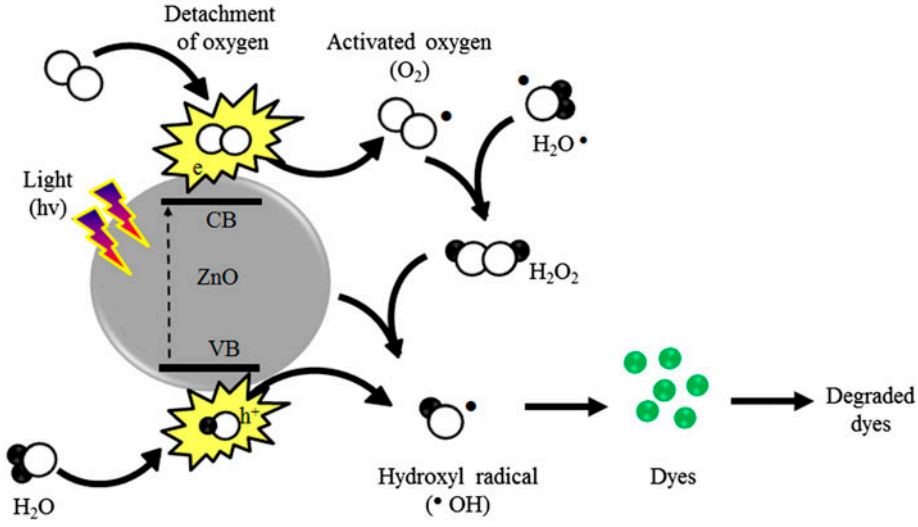

Fig. 1. Proposed photocatalytic degradation mechanism of dyes.

$$\cdot O_2^- + \text{dye} \rightarrow \text{dye} - OO\cdot \quad (6)$$

$$\cdot O_2^- + HO_2^{\cdot} + H^+ \rightarrow H_2O_2 + O_2 \quad (7)$$

Excess H_2O_2 reacts with hydroxyl radicals and holes to produce $HO_2^{\cdot}$ (Eqs. (8) and (9)).

$$H_2O_2 + \cdot OH \rightarrow HO_2^{\cdot} + H_2O \quad (8)$$

$$H_2O_2 + hVB^+ \rightarrow H^+ + HO_2^{\cdot} \quad (9)$$

Electrons in the conduction band are also accountable for the production of hydroxyl radicals (Eqs. (10) and (11)), which have been indicated as the primary cause of organic matter mineralization (Eq. (12)) [25].

$$H_2O_2 + eCB^- \rightarrow \cdot OH + OH^- \quad (10)$$

$$H_2O_2 + \cdot O_2^- \rightarrow \cdot OH + OH^- + O_2 \quad (11)$$

$$\cdot OH + \text{dyes} \rightarrow \text{degraded dyes} \quad (12)$$

2. Materials and methods

2.1. Wastewater characteristics

A dye wastewater sample was collected from the influent sump tank of the central wastewater treatment plant of a newspaper printing factory in Malaysia, named as UMWW. Table 1 shows the chemical properties of UMWW with bluish green of colour apparent at 25°C.

2.2. Synthesis and characterization of ZnO nanoparticles

ZnO nanoparticle (ZnO-PVP-St) was synthesized via a combined precipitation method according to Kanade et al. [17], Behnajady et al. [18] and Lee et al. [26]. The reactant used for this method are oxalic acid dehydrated, zinc acetate dehydrated and Polyvinylpyrrolidone (PVP); all obtained from R&M Marketing, Essex, UK. The precipitation process was conducted under vigorous stirring (3 h) at room temperature (25°C). A furnace (Nabertherm model, Germany) was used for calcination process of the ZnO precipitate under 550°C for 3 h in order to remove impurities. Commercially available ZnO nanoparticle from Sigma Aldrich, USA was used for comparison purposes. Characterizations of the nanoparticles were conducted by X-ray diffractometer (XRD) (Bruker AXS GmbH model) and transmission electron microscopy (TEM) (CM12 Philips model). The purity, crystallinity and morphology of the ZnO-PVP-St and commercial ZnO were shown in Figs. 2 and 3. It was clearly revealed that the nanoparticle used throughout this study contains high purity and crystallinity of ZnO with the nanoparticle size ranging from 7 to 30 nm (ZnO-PVP-St) and 50 to 140 nm (commercial ZnO).

2.3. Membrane and its characterization

Two types of membrane were used in this work: (1) Polypiperazine amide NF membrane (GE Osmonics, Trisep TS40, USA) and (2) Polyamide UF membrane (GE Osmonics, Trisep GMSP, USA). The membrane characteristics are tabulated in Table 2. The observation of membrane surface and cross-sectional morphology was carried out using a field emission scanning electron microscopy (FESEM; Gemini, SUPRA 55VP-ZEISS) equipped with an energy dispersive X-ray (EDX) analysis system. For the cross-sectional analysis, the small pieces of membrane were immersed into liquid nitrogen for 4–5 h. The samples were fractured and dehydrated in an oven under 60°C. Afterwards, the dried samples were gold sputtered for electrical conductivity generating. The observation of the prepared samples was then conducted with the microscope at 3 kV. The intensity of elements on the membrane surface was analysed by the EDX analysis system.

2.4. Experimental set-up and operation

Before starting the experiment, membrane sample with an effective membrane area of 22.90 cm^2 was wetted out by circulating reverse osmosis (RO) water

Table 1
Chemical properties of industrial dye printing wastewater (UMWW)

Chemical properties	Mean value ± standard deviation
COD (mg L^{-1})	1,099 ± 3.0
Turbidity (FAU)	350 ± 5.0
Total suspended solid (TSS) (mg L^{-1})	92.8 ± 3.0
pH	8.0 ± 0.3
Colour intensity (APHA), units	2,406 ± 7.0

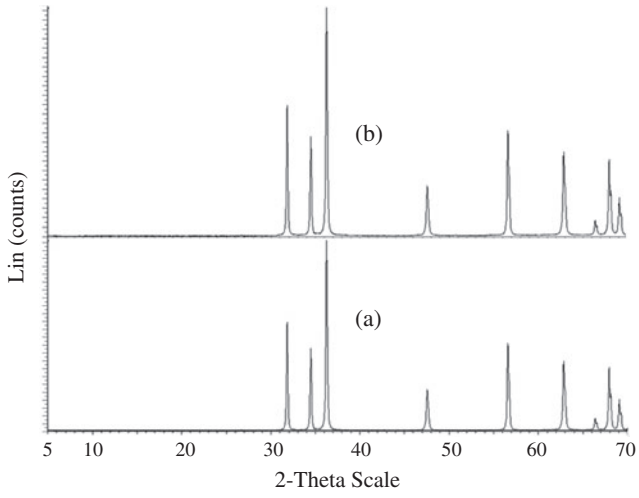

Fig. 2. XRD patterns of (a) commercial ZnO and (b) ZnO-PVP-St.

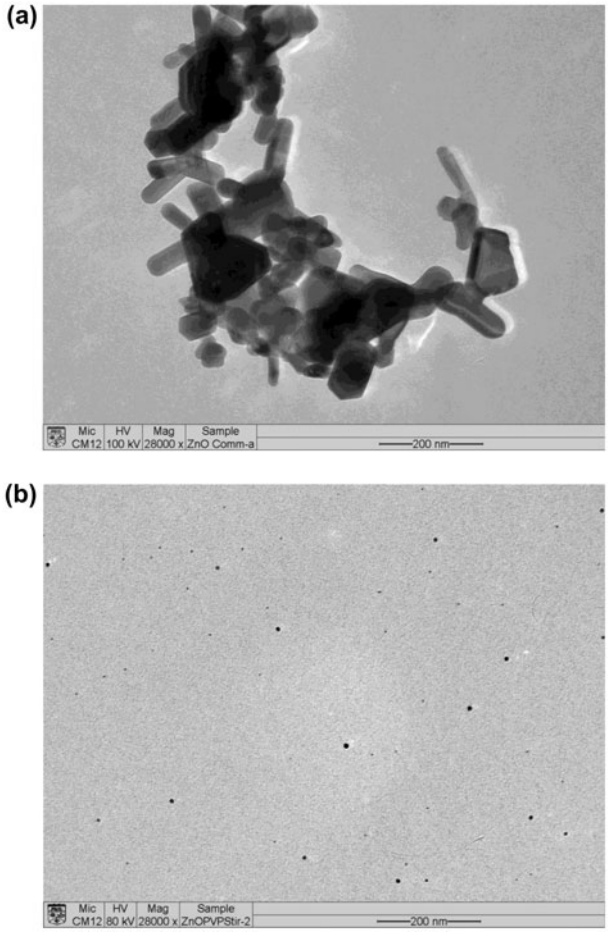

Fig. 3. TEM image of (a) commercial ZnO and (b) ZnO-PVP-St.

in the MPR at 6 bar for 30 min. This procedure is intended to avoid the membrane compaction during the permeation or separation experiments. Fig. 4 shows the schematic diagram of the laboratory-scale MPR used in this work. A UV lamp (253.7 nm, 18 W, GPH295T5L 4PSE, USA) was placed inside the reactor for the photocatalyst activation. The reactor with 5 L of working volume was designed to operate either in batch or continuous methods. ZnO nanoparticle was added into the reactor filled with the wastewater; and the mixture was well agitated by PL111 model of impeller with WiseStir HS-50A overhead stirrer at 300 rpm during the experiments. Furthermore, the temperature was kept constant at approximately 25°C by recirculating cooling water using a water chiller (SP H_2O model). Sodium hydroxide (NaOH) and hydrochloric acid (HCl) solutions (purchased from R&M Marketing, Essex, UK) were used to adjust the solution pH. The treated water after photocatalysis process was then fed to the stainless steel flat sheet membrane module, 9.8 × 9.8 × 5.1 cm using a masterflex peristaltic pump at 6 bar. The volume of permeate was weighed by an electronic balance (AND GF-6100, Japan). Consequently, the weighing data was transferred continuously to a personal computer through a programme installed (RsKey Ver. 1.34). In the first stage of this study, two parameters were examined which are pH values (2.0–11.0) and photocatalyst loading (0.8–1.0 g L^{-1}) in order to determine the optimum operating conditions of the MPR. The optimum operating condition was then applied for the comparison study of different types of ZnO nanoparticles and NF/UF membrane performances.

2.5. Analytical method

A Microprocessor pH metre (Sastec ST-PHS3BW Model) was used for the pH measurements. Colour intensity, chemical oxygen demand (COD) and turbidity of the influent and effluent were measured with a spectrophotometer (HACH DR/2010, USA). Total suspended solid (TSS) of the samples were determined according to the Standard Methods [27].

3. Results and discussion

3.1. Membrane performances

NF and UF membrane performances in the MPR system were investigated using NaCl and Na_2SO_4 (300 mg L^{-1}) solution under 1–6 bar at 25°C. The membranes permeability is determined by plotting the pure water flux and salts flux vs. operation pressure. It was found that the membrane permeability during pure

Table 2
Characteristics of the NF and UF membranes

Membrane characteristics	NF membrane	UF membrane
MWCO (Da)[a]	200	4,000
pH tolerance[a]	2.0–12.0	2.0–11.0
Standard operation pressure (bar)[a]	2.0–14.0	0.1–6.0
Hydrophobicity[b]	Hydrophilic	Hydrophobic
Contact angle (°)[b]	39.0 ± 1.5	60.18 ± 1.37

[a]Information obtained from manufacturer.
[b]Value obtained from experimental measurements.

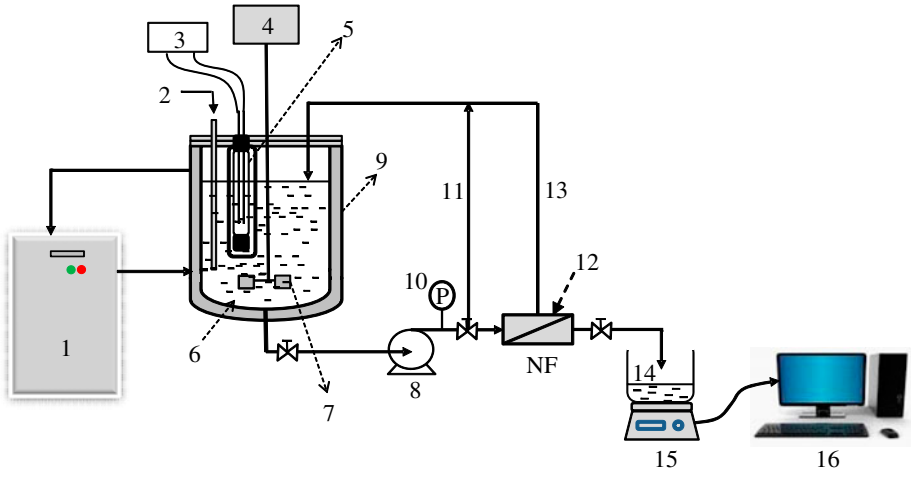

Fig. 4. Schematic diagram of MPR system. (1) Water chiller, (2) feed, (3) power, (4) motor, (5) UV lamp, (6) photocatalytic reactor, (7) agitator, (8) pump, (9) cooling jacket, (10) pressure gauge, (11) bypass flow, (12) membrane filtration system, (13) recycle fow, (14) reservoir tank, (15) electronic balance, and (16) computer.

water filtration for NF and UF membrane was higher than salts filtration in the order of $P_{pure} > P_{Na_2SO_4} > P_{NaCl}$. The values of permeability, r^2 and salts rejections were tabulated in Table 3. For NF process, the rejection of divalent salt Na_2SO_4 were high compared to the monovalent salt NaCl, due to the size of ions and the negatively charged membrane surface [23]. However, UF process presented low rejection performance for the both salts due to the small particles/molecules/ion of salts can pass easily through the UF membranes.

3.2. Effect of initial pH

The effect of pH plays a significant role in controlling the photocatalytic efficiency and fouling behaviour in MPR system [27,28]. The charge of dye molecules, ZnO nanoparticles and membrane surface

Table 3
Performance of NF and UF membranes

Substance	NF membrane			UF membrane		
	Permeability ($Lm^{-2}h^{-1}bar^{-1}$)	r^2	Salt rejection (%)	Permeability ($Lm^{-2}h^{-1}bar^{-1}$)	r^2	Salt rejection (%)
RO water	6.2005	0.9844	–	23.1220	0.9983	–
NaCl	5.2461	0.9763	67	18.1630	0.9883	0
Na_2SO_4	3.6550	0.9939	94	12.2850	0.9942	0

will change depending on the solution pH, which consequently influenced the photocatalytic process and continue to affect the characteristics of membrane during the filtration process [29,30]. In order to investigate the appropriate pH of UMWW in MPR and interactions of membrane–dye–ZnO, the photocatalytic process was performed under various initial pH in the range 2–11, which subsequently moved to the filtration process. It could be noted that the original pH of UMWW was pH 8 from influent stream. The fouling behaviour of NF membrane is shown in Fig. 5, in terms of normalized flux (J/J_o) for easy comparison of the data. The results clearly demonstrate that the permeate flux was responsive to the solution pH.

Gradual flux decline could be clearly seen at the initial two hours of filtration followed by constant flux declines for all the UMWW conditions. The final fluxes in a time span of 8 h were about 10, 14, 6 and 23% of the initial flux for initial pH 2, pH 7, pH 8 and pH 11, respectively. The results were reasonably related to the effectiveness of the photocatalysis process as the pretreatment of wastewater, as revealed in Table 4. Besides, it was also corresponded to the isoelectric point (IEP) of the membrane, ZnO and dye molecules. Since the IEP of NF membrane is ~5.5, the membrane surface will has negative charge for pH > IEP, and conversely has positive charge for pH < IEP. Similarly for the case of ZnO (IEP ~9) and dye molecules (IEP ~5), they will carry positive charges when the solution pH is lower than their IEP. On the contrary, negative charges will predominate when the pH solution is higher than their IEP. The severe fouling at pH 2, 7 and 8 is possibly due to the weakest electrostatic repulsion between the membrane surface, ZnO and the wastewater because all the pH were near to their IEP. The dye and ZnO could easily accumulate and deposited on the membrane surface to form a cake layer. As a result, the flow resistance were increased at pH around the IEP. For solution pH away from the membrane surface (pH 11), the stronger electrostatic repulsion resulted in lesser accumulation and deposition of the dyes and ZnO on the membrane surface. Furthermore, the data in Table 4 also demonstrate that all the chemical properties including COD, turbidity and TSS have reduced by 91, 100 and 95%, respectively. The results revealed that the chemical properties improvement of UMWW was not responsive to the solution pH. Therefore, it can be deduced that the initial pH plays an important role in the MPR for improving the performances of the photocatalytic degradation process which led to reduction of the membrane fouling.

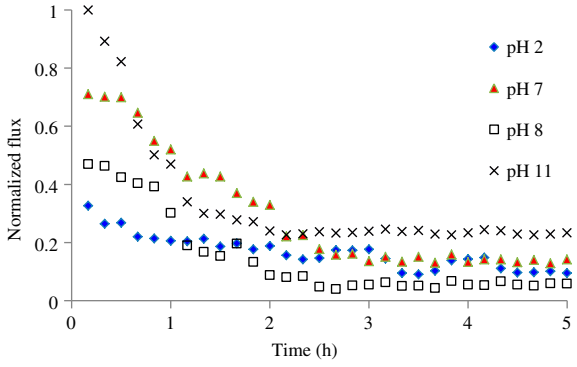

Fig. 5. Normalized flux decline of NF membrane under various pH of UMWW. Test conditions employed were inlet pressure = 6.0 bar, temperature = 25 ℃, photocatalyst = ZnO-PVP-St 0.3 g L^{-1}.

3.3. Effect of ZnO loading

Effect of ZnO-PVP-St loading from 0.08 to 0.50 g L^{-1} in MPR was carried out under pH 11 with constant inlet pressure (6.0 bar) and temperature (25 ℃). It was clearly observed in Fig. 6 that the final normalized membrane flux decreased significantly with the increase of the ZnO loading from 0.10 to 0.50 g L^{-1}. The result was associated with the decreasing of UMWW degraded after the photocatalysis process

Table 4
Characteristics of UMWW after filtration under different initial pH

Solution pH	UMWW degraded after photocatalysis process (%)	UMWW removal after nanofiltration (%)	COD reduction (%)	Turbidity reduction (%)	TSS reduction (%)
2	32	100	90	100	95
7	36	99	91	100	94
8	29	100	91	100	95
11	49	100	91	100	95

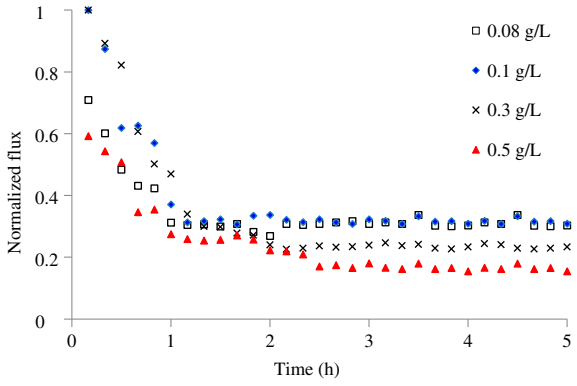

Fig. 6. Normalized flux decline of NF membrane under various ZnO loading. Test conditions employed were inlet pressure = 6.0 bar, temperature = 25°C, pH 11, photocatalyst = ZnO-PVP-St.

(Table 5), as described previously. According to Wang et al. [31], enhancement of photocatalyst loading can cause the obstruction of UV light adsorption, since the photocatalyst is easier to be overlapped. In case of 0.08 g L^{-1} of ZnO-PVP-St loading, severe decrease in normalized flux was observed for the first 2 h, but almost the same final normalized flux was achieved in the case of 0.10 g L^{-1} of ZnO loading (Fig. 6). This phenomenon is related to the photocatalytic degradation results (Table 5), since there was an optimum amount of photocatalyst loading under different experimental conditions [32]. In addition, the effective surface of ZnO-PVP-St and adsorption of UV light during the photocatalysis process also influence the degradation process which affected the fouling of NF membrane. Similar with the case of different initial pH (Section 3.2), the improvement of UMWW chemical properties was also not responsive to the ZnO loading with 92% of COD reduction, 100% of turbidity reduction and 95% of TSS reduction as shown in Table 5.

3.4. Effect of presence/absence of ZnO and different types of ZnO

In order to study the efficiency of ZnO-PVP-St in the MPR, the experiments were carried out in the absence of photocatalyst and presence of commercial ZnO for comparison purposes. As revealed in Fig. 7, the order of normalized flux decline was No ZnO > Commercial ZnO > ZnO-PVP-St. The outcome verified that the photocatalysis process has facilitated to reduce membrane fouling in MPR. Furthermore, ZnO-PVP-St showed better performance in terms of the photocatalysis process (Table 6), reducing membrane fouling (Fig. 7) and improvement of UMWW chemical properties (Table 6). The possible explanation for these results might be the effect of size and preparation method of the photocatalyst. It has been noted in section 2.2 that the size of ZnO-PVP-St is about 10 times smaller than commercial ZnO (Fig. 3). Due to the decrease of ZnO size, the surface area of ZnO

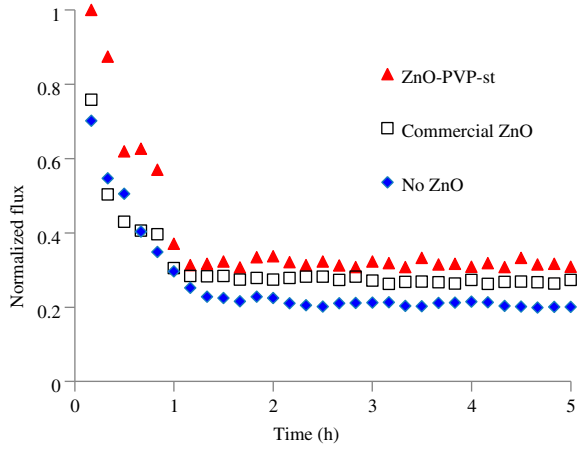

Fig. 7. Normalized flux decline of NF membrane with the presence/absence of ZnO and different types of ZnO. Test conditions employed were inlet pressure = 6.0 bar, temperature = 25°C, pH 11, photocatalyst = 0.10 g L^{-1}.

Table 5
Characteristics of UMWW after filtration under various ZnO loading

ZnO loading (g L^{-1})	Dye degraded after photocatalysis process (%)	Dye removal after nanofiltration (%)	COD reduction (%)	Turbidity reduction (%)	TSS reduction (%)
0.08	58	100	92	100	94
0.10	68	100	92	100	94
0.30	49	100	91	100	95
0.50	40	100	92	100	95

Table 6
Characteristics of UMWW after filtration under the presence/absence of ZnO and different types of ZnO

Types of ZnO	Dye degraded after photocatalysis process (%)	Dye removal after nanofiltration (%)	COD reduction (%)	Turbidity reduction (%)	TSS reduction (%)
ZnO-PVP-St	68	100	92	100	94
Commercial ZnO	42	100	88	98	88
No ZnO	–	100	88	98	86

photocatalyst will increase and lead to enhancement of the photoexcitation of ZnO-PVP-St. This resulted in high performance of photocatalytic degradation process and subsequently improvement of the NF process. In addition, there are a lot of structural defects in commercial ZnO, which may reduce the effectiveness of degradation process and consequently affected the NF process. This is due to the preparation method of commercial ZnO, which was the main feature which affected the photocatalytic activity [31].

3.5. Effect of different types of membrane

Polypiperazine amide (NF) and polyamide (UF) membranes were used in the MPR to investigate their performances for UMWW treatment under the same trans-membrane pressure, 6 bar. Fig. 8 shows the behaviour of volume treated in 5 h of time span using NF and UF membrane. It could be seen that higher volume of UMWW was treated by UF membrane at the initial time of filtration (~37 mL), however, it was rapidly decreases within 30 min followed by gradual volume declines before reaching the constant relatively low volume at ~2 mL. The result was likely attributed to the pore blocking effect which was caused by the rapid formation of cake layer on the membrane surface [33]. In the case of NF, it began with lower volume treated (~20 mL) and gradually decreases within two hours of time span. This is due to a starting of a concentration polarization effect caused by the solutes on the NF membrane surface [34]. The constant volume treated (~6 mL) was reached, may be attributed to both the pore blocking and concentration polarization effects [33].

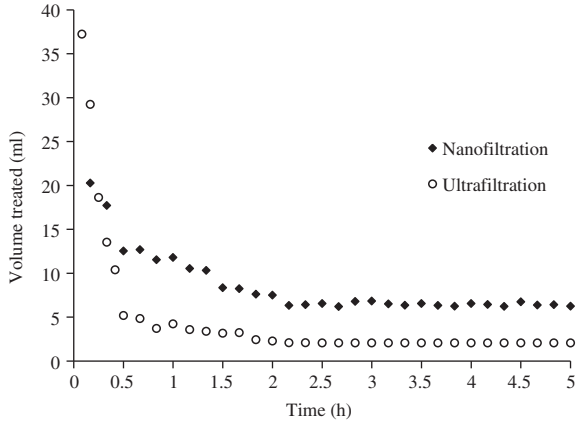

Fig. 8. Volume treated after filtration using NF and UF membrane in MPR. Test conditions employed were inlet pressure = 6.0 bar, temperature = 25°C, pH 11, photocatalyst = ZnO-PVP-St 0.10 g L^{-1}.

The influence of NF and UF membrane on dye removal, COD, turbidity and TSS reduction is shown in Table 7. It can be clearly seen that all the retention is more noticeable for NF membranes than for UF. The results were expected since the low molecular weight and soluble dyes (acid, reactive, basic, etc.) cannot be removed by an UF process [35,36]. The result also confirmed that the small particles/molecules/ion can pass easily through the UF membrane. Therefore, NF was shown to be the appropriate technique in the MPR for dye wastewater treatment.

3.5.1. FESEM and EDX analysis

FESEM images and EDX analysis of fresh and fouled NF and UF membrane after filtration in the presence of ZnO-PVP-St photocatalyst are shown in Fig. 9 and Table 8. It was clearly observed that both the membranes after the filtration process have many contaminants entrapped on the surface, obviously referring to the chemical elements in UMWW and ZnO-PVP-St as confirmed in EDX analysis. However, the percentage of the elements and ZnO retained on the NF membrane surface were higher in comparison to UF (Table 8). This is also in accordance with the earlier observations in previous section, which showed that the low molecular weight, soluble dyes and small molecules/ions would be transported in the permeate

Table 7
Characteristics of UMWW after filtration under different types of membrane

Types of membrane	Dye degraded after photocatalysis process (%)	Dye removal after filtration (%)	COD reduction (%)	Turbidity reduction (%)	TSS reduction (%)
NF	68	100	92	100	94
UF	68	73	12	41	52

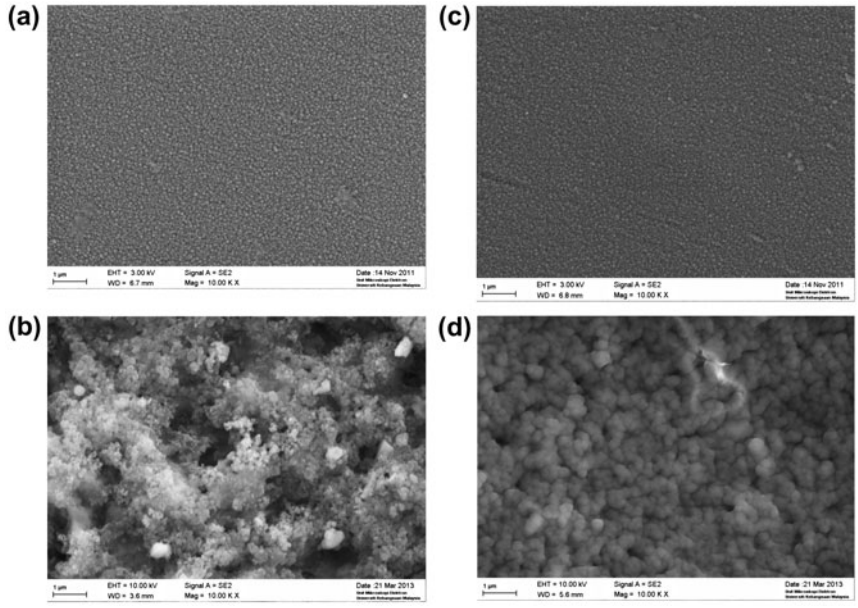

Fig. 9. Membrane surface FESEM image of (a) Fresh NF membrane, (b) Fouled NF membrane, (c) Fresh UF membrane, and (d) Fouled UF membrane.

Table 8
EDX analysis of NF and UF membrane

Condition/element	Fresh NF (%)	Fouled NF (%)	Fresh UF (%)	Fouled UF (%)
Carbon (C)	78.52	52.50	78.49	75.29
Oxygen (O)	18.27	33.37	18.24	20.09
Sodium (Na)	0.18	–	0.21	–
Sulphur (S)	3.03	0.29	3.06	0.29
Magnesium (Mg)		0.42		0.23
Aluminium (Al)		0.64		0.33
Silicon (Si)		2.61		1.35
Phosphorus (P)		1.07		0.65
Potassium (K)		0.47		0.10
Calcium (Ca)		1.91		0.76
Iron (Fe)		0.26		–
Zinc (Zn)		6.47		0.90

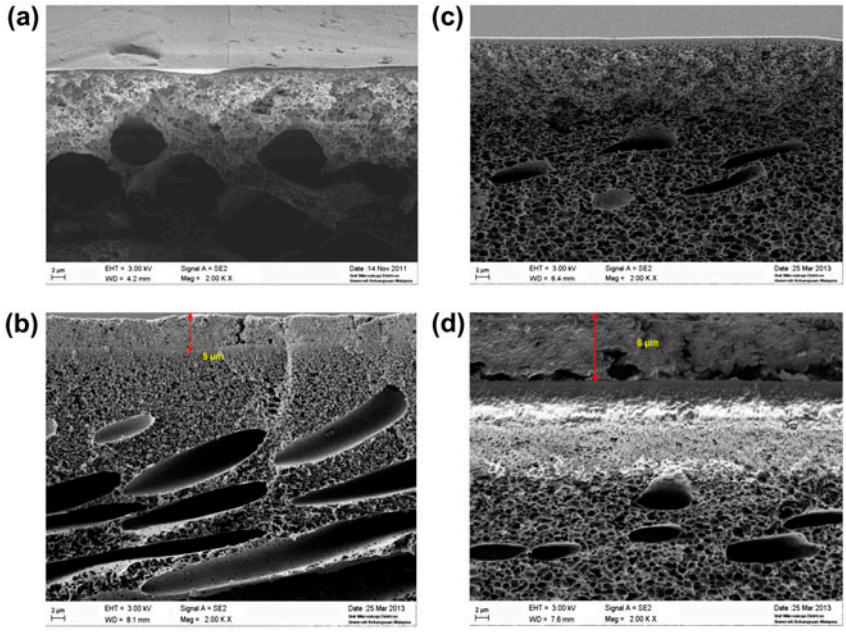

Fig. 10. Cross section FESEM image of (a) Fresh NF membrane, (b) Fouled NF membrane, (c) Fresh UF membrane, and (d) Fouled UF membrane.

flow. Moreover, the cross-section FESEM image (Fig. 10) revealed that the fouling layer cake was formed on the both of membrane surface. The cake layer is thicker on UF surface (8 μm) in comparison to NF surface (5 μm). This was believed to be the primary source which leads to severe fouling for the UF membrane.

4. Conclusions

The industrial newsprint wastewater (UMWW) was successfully treated using MPR with utilization of self-synthesized ZnO nanoparticles via precipitation method. It was found that pH 11 and 0.1 g L^{-1} of ZnO loading were the optimum operational condition of the MPR. However, the effluent chemical properties were not responsive to the effect of various pH and ZnO loading. Performances of NF membrane and the chemical properties of effluent were improved in the presence of ZnO-PVP-St as the photocatalyst in the MPR. From the results, NF membrane was shown to be the appropriate technique in the MPR due to the dye molecules and ZnO nanoparticles could pass through the UF membrane. The membrane characterizations results confirmed that ZnO-PVP-St nanoparticles and NF membrane have a great potential in MPR for industrial dye wastewater treatment.

Acknowledgements

The authors gratefully acknowledge the financial support from Universiti Kebangsaan Malaysia via grant UKMGUP-2011-033 and from the Ministry of Higher Education Malaysia (MOHE) for its financial and administrative supports. The authors would like to express their thanks to the newspaper printing factory in Selangor, Malaysia for providing the industrial dye wastewater for this work.

References

[1] X. Zheng, J. Liu, Dyeing and printing wastewater treatment using a membrane bioreactor with a gravity drain, Desalination 190 (2006) 277–286.
[2] Ch. Huang, Y.Y. Liu, Y. Luo, X.P. Lou, Research status of dyeing wastewater treatment, Nat. Sci. Ed. 6 (2001) 139–142.
[3] A.Y. Zahrim, C. Tizaoui, N. Hilal, Evaluation of several commercial synthetic polymers as flocculant aids for removal of highly concentrated C.I. Acid Black 210 dye, J. Hazard. Mater. 182 (2010) 624–630.
[4] G. Yang, Z. Yan, T. Xiao, B. Yang, Low-temperature synthesis of alkalis doped TiO_2 photocatalysts and their photocatalytic performance for degradation of methyl orange, J. Alloys Compd. 580 (2013) 15–22.
[5] S. Wang, D. Li, C. Sun, S. Yang, Y. Guan, H. He, Synthesis and characterization of g-C_3N_4/Ag_3VO_4 composites with significantly enhanced visible-light photocatalytic activity for triphenylmethane dye degradation, Appl. Catal., B 144 (2014) 885–892.

[6] T. Sreethawong, S. Ngamsinlapasathian, S. Yoshikawa, Surfactant-aided sol–gel synthesis of mesoporous-assembled TiO_2–NiO mixed oxide nanocrystals and their photocatalytic azo dye degradation activity, Chem. Eng. J. 192 (2012) 292–300.
[7] S. Mozia, Photocatalytic membrane reactors (PMRs) in water and wastewater treatment. A review, Sep. Purif. Technol. 73 (2010) 71–91.
[8] R. Molinari, L. Palmisano, E. Drioli, M. Schiavello, Studies on various reactor configurations for coupling photocatalysis and membrane processes in water purification, J. Membr. Sci. 206 (2002) 399–415.
[9] P. Cui, X. Zhao, M. Zhou, L. Wang, Photocatalysis-membrane separation coupling reactor and its application, Chin. J. Catal. 27 (2006) 752–754.
[10] K.-H. Choo, R. Tao, M.-J. Kim, Use of a photocatalytic membrane reactor for the removal of natural organic matter in water: Effect of photoinduced desorption and ferrihydrite adsorption, J. Membr. Sci. 322 (2008) 368–374.
[11] R.A. Damodar, S.-J. You, Performance of an integrated membrane photocatalytic reactor for the removal of Reactive Black 5, Sep. Purif. Technol. 71 (2010) 44–49.
[12] S. Yang, J.-S. Gu, H.-Y. Yu, J. Zhou, S.-F. Li, X.-M. Wu, L. Wang, Polypropylene membrane surface modification by RAFT grafting polymerization and TiO_2 photocatalysts immobilization for phenol decomposition in a photocatalytic membrane reactor, Sep. Purif. Technol. 83 (2011) 157–165.
[13] S.K. Kansal, M. Singh, D. Sud, Studies on photodegradation of two commercial dyes in aqueous phase using different photocatalysts, J. Hazard. Mater. 141 (2007) 581–590.
[14] S. Sakthivel, B. Neppolian, M.V. Shankar, B. Arabindoo, M. Palanichamy, V. Murugesan, Solar photocatalytic degradation of azo dye: Comparison of photocatalytic efficiency of ZnO and TiO, Sol. Energ. Mat. Solo. C. 2(77) (2003) 65–82.
[15] J. Xie, Y. Li, W. Zhao, L. Bian, Y. Wei, Simple fabrication and photocatalytic activity of ZnO particles with different morphologies, Powder Technol. 207 (2011) 140–144.
[16] J.-H. Sun, S.-Y. Dong, Y.-K. Wang, S.-P. Sun, Preparation and photocatalytic property of a novel dumbbell-shaped ZnO microcrystal photocatalyst, J. Hazard. Mater. 172 (2009) 1520–1526.
[17] K.G. Kanade, B.B. Kale, R.C. Aiyer, B.K. Das, Effect of solvents on the synthesis of nano-size zinc oxide and its properties, Mater. Res. Bull. 41 (2006) 590–600.
[18] M.A. Behnajady, N. Modirshahla, E. Ghazalian, Synthesis of ZnO nanoparticles at different conditions: A comparison of photocatalytic activity, Dig. J. Nanomater. Biostructures 6 (2011) 467–474.
[19] X.-L. Hu, Y.-J. Zhu, S.-W. Wang, Sonochemical and microwave-assisted synthesis of linked single-crystalline ZnO rods, Mater. Chem. Phys. 88 (2004) 421–426.
[20] K. Nomura, N. Shibata, M. Maeda, Orientation control of zinc oxide films by pulsed current electrolysis, J. Cryst. Growth 235 (2002) 224–228.
[21] T. Sekiguchi, S. Miyashita, K. Obara, T. Shishido, N. Sakagami, Hydrothermal growth of ZnO single crystals and their optical characterization, J. Cryst. Growth 214–215 (2000) 72–76.
[22] J. Xiang, Z. Xie, M. Hoang, K. Zhang, Effect of amine salt surfactants on the performance of thin film composite poly(piperazine-amide) nanofiltration membranes, Desalination 315 (2013) 156–163.
[23] M. Jahanshahi, A. Rahimpour, M. Peyravi, Developing thin film composite poly(piperazine-amide) and poly (vinyl-alcohol) nanofiltration membranes, Desalination 257 (2010) 129–136.
[24] C. Kong, T. Shintani, T. Kamada, V. Freger, T. Tsuru, Co-solvent-mediated synthesis of thin polyamide membranes, J. Membr. Sci. 384 (2011) 10–16.
[25] N. Daneshvar, D. Salari, A. Khataee, Photocatalytic degradation of azo dye Acid Red 14 in water on ZnO as an alternative catalyst to TiO_2, J. Photochem. Photobiol., A 162 (2004) 317–322.
[26] S. Lee, S. Jeong, D. Kim, S. Hwang, M. Jeon, ZnO nanoparticles with controlled shapes and sizes prepared using a simple polyol synthesis, Superlattices Microstruct. 43 (2008) 330–339.
[27] National Environment Protection Agency, PR, China, Standard Methods for the Examination of Water and Wastewater, 3rd ed., China Environmental Science Press, Beijing, 1998.
[28] J. Mendret, M. Hatat-Fraile, M. Rivallin, S. Brosillon, Influence of solution pH on the performance of photocatalytic membranes during dead-end filtration, Sep. Purif. Technol. 118 (2013) 406–414.
[29] V.C. Sarasidis, K.V. Plakas, S.I. Patsios, A.J. Karabelas, Investigation of diclofenac degradation in a continuous photo-catalytic membrane reactor. Influence of operating parameters, Chem. Eng. J. 239 (2014) 299–311.
[30] M.D. Afonso, R. Bórquez, Review of the treatment of seafood processing wastewaters and recovery of proteins therein by membrane separation processes—Prospects of the ultrafiltration of wastewaters from the fish meal industry, Desalination 142 (2002) 29–45.
[31] H. Wang, C. Xie, W. Zhang, S. Cai, Z. Yang, Y. Gui, Comparison of dye degradation efficiency using ZnO powders with various size scales, J. Hazard. Mater. 141 (2007) 645–652.
[32] A. Akyol, H.C. Yatmaz, M. Bayramoglu, Photocatalytic decolorization of Remazol Red RR in aqueous ZnO suspensions, Appl. Catal., B 54 (2004) 19–24.
[33] A. Aouni, C. Fersi, B. Cuartas-Uribe, A. Bes-Pía, M.I. Alcaina-Miranda, M. Dhahbi, Reactive dyes rejection and textile effluent treatment study using ultrafiltration and nanofiltration processes, Desalination 297 (2012) 87–96.
[34] Y. He, G. Li, H. Wang, J. Zhao, H. Su, Q. Huang, Effect of operating conditions on separation performance of reactive dye solution with membrane process, J. Membr. Sci. 321 (2008) 183–189.
[35] A. Akbari, J.C. Remigy, P. Aptel, Treatment of textile dye effluent using a polyamide-based nanofiltration membrane, Chem. Eng. Process. 41 (2002) 601–609.
[36] C. Fersi, L. Gzara, M. Dhahbi, Treatment of textile effluents by membrane technologies, Desalination 185 (2005) 399–409.